

# Experimental resin-based dual-cured calcium aluminate and calcium titanate materials for vital pulp therapy

Fabiano Paiva VIEIRA<sup>(a)</sup>   
Alcides GONINI JÚNIOR<sup>(b)</sup>   
Evandro PIVA<sup>(c)</sup>   
Héllen de Lacerda OLIVEIRA<sup>(d)</sup>   
Wellington Luiz de Oliveira DA ROSA<sup>(e)</sup>   
Adriana Fernandes DA SILVA<sup>(c)</sup>   
Rafael Pino VITTI<sup>(e)</sup>   
Cesar Henrique ZANCHI<sup>(c)</sup>   
Sergio da Silva CAVA<sup>(f)</sup> 

<sup>(a)</sup>Instituto Federal de Goiás, Department of Academic Areas, Formosa, GO, Brazil.

<sup>(b)</sup>Universidade Estadual de Londrina, School of Dentistry, Londrina, PR, Brazil.

<sup>(c)</sup>Universidade Federal de Pelotas – UFPes, School of Dentistry, Department of Restorative Dentistry, Pelotas, RS, Brazil.

<sup>(d)</sup>Faculdade Sobres, School of Dentistry, Santa Maria, RS, Brazil.

<sup>(e)</sup>School of Dentistry, Herminio Ometto University Center, Araras, SP, Brazil.

<sup>(f)</sup>Universidade Federal de Pelotas – UFPes, Materials Engineering Graduate Program, Advanced Crystal Growth and Photonics, Pelotas, RS, Brazil.

**Declaration of Interests:** The authors certify that they have no commercial or associative interest that represents a conflict of interest in connection with the manuscript.

## Corresponding Author:

Wellington Luiz de Oliveira da Rosa  
E-mail: darosa.wlo@gmail.com

<https://doi.org/10.1590/1807-3107bor-2022.vol36.0037>

Submitted: February 9, 2021

Accepted for publication: May 3, 2021

Last revision: November 14, 2021

**Abstract:** This paper evaluates the physicochemical and biological properties of experimental resin-based dual-cured calcium aluminate (CA) and calcium titanate (CTi) materials for vital pulp therapy (VPT). The experimental dual-cured materials were obtained as two pastes: a) Bis-EMA 10, PEG 400, DHEPT, EDAB, camphorquinone, and butylated hydroxytoluene; and b) fluoride ytterbium, Bis-EMA 10, Bis-EMA 30, benzoyl peroxide, and butylated hydroxytoluene. The materials were divided into six groups based on the added calcium component: MTA (MTA<sup>®</sup>, Angelus); CLQ (Clinker-Fillapex<sup>®</sup>, Angelus); CA (calcined at 1200°C in pastes a and b); CA800 (calcined at 800°C in paste a); CA1200 (calcined at 1,200°C in paste a); and CTi (paste a). The real-time degree of conversion and rate of polymerization (n = 3), diametral tensile strength (n = 10), hydrogen potential (n = 15), calcium ion release (n = 10), water sorption and solubility (n = 10), and cell viability (n = 6) were evaluated. One- and two-way ANOVA and Tukey's *post hoc* test were used in the analysis of the parametric data, and Kruskal-Wallis and Dunn's multiple tests were used to analyze the nonparametric data ( $\alpha = 0.05$ ). CLQ, CA800 and CA1200 had the highest diametral tensile strength. The water solubility of MTA was similar to that of CA800, CA1200 and CTi. CA800 and CA1200 resulted in cell viabilities similar to those of MTA and CLQ. The experimental dual-cured CA-based material that calcined at 800°C showed physicochemical and biological properties suitable for VPT, and similar to those of MTA.

**Keywords:** Cytotoxins; Dental Pulp Capping; Dental Pulp Exposure; Pulp Capping and Pulpectomy Agents; Dental Materials.

## Introduction

The ability to maintain pulp tissue sound after deep carious lesions and traumatic or iatrogenic injuries continues to pose a challenge to clinicians.<sup>1,2</sup> Treatments based on vital pulp therapies (VPTs), such as pulp capping, can be performed to avoid extensive treatment, maintain pulp vitality and improve tooth survival.<sup>3,4</sup> VPT consists of placing a pulp capping agent directly over the exposed pulp (direct pulp capping), or a cavity liner or sealer above the residual caries lesion (indirect pulp capping).<sup>4</sup>

Several pulp capping materials can be used for VPT, such as calcium hydroxide cements, mineral trioxide aggregate (MTA), and biomaterials



derived from MTA (calcium silicate, calcium phosphate and calcium aluminate-based materials).<sup>4,5</sup> Calcium hydroxide cements are widely used, but their long-term solubility and gradual disintegration are their main drawbacks.<sup>6,7</sup> MTA was developed to counter the limitations of calcium hydroxide cements. The properties of MTA are dependent on humidity,<sup>8</sup> and have improved mechanical properties in wet environments.<sup>9</sup> MTA is a Portland cement-based formulation composed mainly of tricalcium silicate, tricalcium aluminate, bismuth oxide and tetracalcium aluminoferrite.<sup>1-10</sup> Calcium release may improve the antibacterial properties, dentinogenesis, and apatite formation.<sup>7-11</sup> Some recent studies have shown that MTA is the material with the best physicochemical and biological properties for VPT.<sup>4,12-14</sup>

However, researchers have worked to improve the physicochemical and handling properties of biomaterials derived from MTA.<sup>4,5</sup> Experimental light-cured MTA materials have been developed with physicochemical properties similar to those of conventional MTA, but with shorter working times (photoactivation time: 20-60 s).<sup>15-17</sup> Furthermore, the resin-based materials used in VPT have the additional advantage of allowing chemical bonding with the resin composite, which could decrease the failures at the capping-restorative material interface.<sup>17</sup> Some studies have shown that even a light-cured calcium silicate-based material for pulp capping (TheraCal<sup>®</sup>, Bisco, Schaumburg, IL, USA) could have suitable calcium-release ability after polymerization.<sup>7,18,19</sup> The ability of calcium hydroxide to disassociate into calcium and hydroxyl ions could lead to alkalization of the environment, and improve the bioactive properties, including apatite formation, followed by new dentin production, as well as cell growth and proliferation.<sup>7,18</sup> A recent clinical study showed that the clinical success (maintenance of pulp vitality) of the light-cured calcium silicate-based material (TheraCal<sup>®</sup>) was similar to that of MTA applied by direct pulp capping of primary molars after 12 months.<sup>7</sup> Moreover, the incorporation of calcium aluminate or calcium titanate into pulp capping materials may enhance the hydration reaction, and result in a continuous process of dissolution and precipitation, as well as enhanced reparative ability of the material.<sup>20-21</sup> On

the other hand, studies have revealed the molecular toxicity of substances released by resin-based dental materials, given that some monomers can cause cytotoxic and genotoxic effects in the oral cavity.<sup>22</sup>

To solve this problem, new monomers have been proposed that can reduce diffusion of the monomer through dentin, and improve the biocompatibility of resin-based dental materials.<sup>17,23,24</sup> Despite several optional materials, none seems ideal for VPT. Thus, the development of new VPT-targeted materials able to incorporate all the properties required for optimal performance seems to be an interesting strategy to offset the limitations of currently available materials.

Therefore, this study aimed to develop and evaluate the biological and physicochemical properties of experimental dual-cured calcium aluminate- and calcium titanate-based materials designed for VPT. The null hypothesis is that the biological and physicochemical properties of the experimental materials are similar to those of commercial materials.

## Methodology

### Study design and formulation of experimental materials

Two types of materials (calcium aluminate and calcium titanate) were synthesized using chemical methods. Then, the two synthesized materials were subjected to heat treatments at different temperatures. Calcium aluminates (CA) CA800 and CA1200 were synthesized and heat-treated at 800°C and 1200°C, respectively. Calcium titanate (CTi) was synthesized and heat-treated at 700°C. These three samples were incorporated into resin composites in two pastes.

All the commercial and experimental materials evaluated are presented in Table 1. Experimental resin-based materials were composed of two blended pastes. The following six groups were evaluated: MTA (MTA<sup>®</sup>, Angelus, Londrina, PR, Brazil; commercial reference); CLQ (Clinker-Fillapex<sup>®</sup>, Angelus); CA (with 60% of calcium aluminate -  $3\text{CaO}\cdot\text{Al}_2\text{O}_3$  - calcined at 1200°C in two pastes); CA800 (with 60% of CA calcined at 800°C in one paste); CA1200 (with 60% of CA calcined at 1200°C in one paste); and CTi (with 60% of calcium titanate -  $\text{CaTiO}_3$  - in one paste). Fluoride ytterbium was used as a radiopacifier in the CA 800, CA1200 and

CTi groups. The MTA (chemical setting) samples were mixed at a 3:1 ratio (powder/liquid) according to the manufacturer's instructions, while the other materials (dual curing in two pastes) were used at 1:1 ratios.

CA and CTi were used as inorganic filler particles in the experimental groups. Calcium nitrate tetrahydrate (Ca(NO<sub>3</sub>)<sub>2</sub>•4H<sub>2</sub>O), aluminum nitrate nonahydrate (Al(NO<sub>3</sub>)<sub>3</sub>•9H<sub>2</sub>O) and urea (CO(NH<sub>2</sub>)<sub>2</sub>) were used as fuels to produce CA. These two reagents and the fuel were obtained from Sigma-Aldrich (St. Louis, USA), and used without any further treatment. The amount of each component required for the chemical reaction to produce tricalcium aluminate was calculated based on the total valences of oxidizing and reducing reagents, and on the fuel. These reagents were previously weighed on a hot plate, placed on a heating plate at 90°C, and subsequently transferred to a preheated muffle furnace at 400°C. The material obtained after this reaction was heat-treated at 800°C or 1200°C for 4 h to promote the formation of CA crystalline phases. A 45-µm sieve was used to remove the filler particle agglomerates obtained at the end of this process, as previously published.<sup>25,26</sup>

Titanium isopropoxide [Ti(OC<sub>3</sub>H<sub>7</sub>)<sub>4</sub>] (Vetec, Duque de Caxias, Brazil), absolute ethyl alcohol (Vetec), anhydrous citric acid (C<sub>6</sub>H<sub>8</sub>O<sub>7</sub>) (Synth, Diadema, SP, Brazil), calcium nitrate tetrahydrate (Ca(NO<sub>3</sub>)<sub>2</sub>•4H<sub>2</sub>O) (Sigma-Aldrich), and ethylene glycol (C<sub>2</sub>H<sub>6</sub>O<sub>2</sub>) (Vetec) were used to produce calcium titanate. Stoichiometric calculations determined the required amount of each element to be used in the chemical reaction to yield calcium titanate. The citric acid/ethylene glycol mass ratio was 60:40.<sup>27</sup>

The amount of each reagent was weighed, and added to a beaker placed on a heating plate under constant agitation, in the same sequence as that used for the reagents, as described above. Then, each reagent was slowly heated to 100°C to promote citrate polymerization by a polyesterification reaction to evaporate the solvent and adjust the viscosity. The material obtained (a polymeric resin) was placed in a conventional furnace at 300°C for 2 h at a heating rate of 1°C/min, which promoted both the pulverization of the polymeric resin, and the formation of the precursor powder. Finally, these materials were heat-treated in a microwave oven at 700°C for 7 h at a heating rate of

**Table 1.** Chemical composition of the materials tested.

Material	Composition
MTA® (Angelus)	Powder: Portland cement, tricalcium silicate, dicalcium silicate, tricalcium aluminate, tetracalcium iron aluminate, bismuth oxide. Liquid: distilled water.
CLQ (CDC-Bio)	Paste A: 60% clinker-Fillapex Angelus®, 20% Bis-EMA 10, 20% PEG 400, 1% DHEPT, 0.8% EDAB, 0.4% CQ, 0.05% butylated hydroxytoluene Paste B: 60% fluoride ytterbium, 20% Bis-EMA 10, 20% Bis-EMA 30, 1.5% benzoyl peroxide, 0.05% butylated hydroxytoluene
CA (CDC-Bio)	Paste A: 60% CA (1200°C), 20% Bis-EMA 10, 20% PEG 400, 1% DHEPT, 0.8% EDAB, 0.4% CQ, 0.05% butylated hydroxytoluene Paste B: 60% CA (1200°C), 20% Bis-EMA 10, 20% Bis-EMA 30, 1.5% benzoyl peroxide, 0.05% butylated hydroxytoluene
CA800 (CDC-Bio)	Paste A: 60% CA (800°C), 20% Bis-EMA 10, 20% PEG 400, 1% DHEPT, 0.8% EDAB, 0.4% CQ, 0.05% butylated hydroxytoluene Paste B: 60% fluoride ytterbium, 20% Bis-EMA 10, 20% Bis-EMA 30, 1.5% benzoyl peroxide, 0.05% butylated hydroxytoluene
CA1200 (CDC-Bio)	Paste A: 60% CA (1200°C), 20% Bis-EMA 10, 20% PEG 400, 1% DHEPT, 0.8% EDAB, 0.4% CQ, 0.05% butylated hydroxytoluene Paste B: 60% fluoride ytterbium, 20% Bis-EMA 10, 20% Bis-EMA 30, 1.5% benzoyl peroxide, 0.05% butylated hydroxytoluene
CTi (CDC-Bio)	Paste A: 60% calcium titanate, 20% Bis-EMA 10, 20% PEG 400, 1% DHEPT, 0.8% EDAB, 0.4% CQ, 0.05% butylated hydroxytoluene Paste B: 60% fluoride ytterbium, 20% Bis-EMA 10, 20% Bis-EMA 30, 1.5% benzoyl peroxide, 0.05% butylated hydroxytoluene

MTA: mineral trioxide aggregate. Bis-EMA: diether dimethacrylate. PEG 400: polyethylene glycol (400) dimethacrylate. DHEPT: dihydroxyethyl p-toluidine. EDAB: Ethyl 4-(dimethylamino)benzoate. CQ: camphorquinone. CA: calcium aluminate. CDC-Bio: Center for Development and Control of Biomaterials.

20°C/min to obtain the filler particles. A 45- $\mu\text{m}$  sieve was used to remove the filler particle agglomerates obtained at the end of the process described above.

### **X-ray diffraction analysis (XRD), Fourier transform infrared (FTIR) spectroscopy, energy-dispersive X-ray (EDX) spectroscopy and scanning electron microscopy (SEM)**

The filler particles were characterized by XRD, FTIR, EDX and SEM. The crystalline phase analysis using XRD was carried out using the Rigaku D/Max2500 PC diffractometer (Rigaku Corporation, Tokyo, Japan) and Cu K $\alpha$  radiation at 30 mA and 30 kV, with detector rotations between 10° and 80°, a sampling pitch of 0.02°, and a scan speed of 2°/min. The materials were analyzed using an FTIR spectrometer (Shimadzu Prestige21 Spectrometer, Shimadzu, Kyoto, Japan) with Happ-Genzel apodization at a range of 4000 and 600  $\text{cm}^{-1}$ , and at a spectral resolution of 4  $\text{cm}^{-1}$ , with 10 scans per spectrum. The background noise was removed prior to analysis by conducting background scans. The elemental constitution of each phase identified was determined by EDX analysis using a fluorescence spectrometer (Shimadzu, Japan). The filler particles were visualized by SEM (5400, JEOL, Tokyo, Japan), and the particle microstructure, typical particle agglomerates and grain morphology were assessed in the backscatter electron mode at 1000x magnification.

### **Kinetics of polymerization**

The degree of conversion (DC) of the experimental materials was evaluated using real-time Fourier transform infrared spectroscopy-attenuated total reflectance (FTIR-ATR) spectroscopy (ZnSe crystal, PIKE Technologies, Madison, USA). A support was used to control the distance between the fiber tip of the light-curing unit (LED, Radian® Curing Light, SDI, Bayswater, Victoria, Australia) and the sample, at 5 mm. Light-curing of each material ( $n = 3$ ) was performed at 1400  $\text{mW}/\text{cm}^2$ . The IRSolution software (Shimadzu) program was used for Happ-Genzel apodization, at a range of 1750 and 1550  $\text{cm}^{-1}$ , at a resolution of 4  $\text{cm}^{-1}$  and a mirror-speed of 2.8  $\text{mm}/\text{s}$ , and at monitoring mode during photoactivation;

the scans were conducted every 1 s. A standardized amount of the sample (0.1 g) was manipulated for 60 s and dispensed directly onto the ZnSe crystal. Then, an initial scan was performed before light-curing and sample-scanning for 60 s. DC was calculated considering the intensity of the carbon-carbon double-bond stretching vibration (peak height) at 1635  $\text{cm}^{-1}$ . The internal standard consisted of stretching the symmetric ring at 1610  $\text{cm}^{-1}$  from the polymerized and unpolymerized samples. The plotted data were analyzed by means of curve-fitting, and a logistic nonlinear regression was performed. Data fitting was used to calculate the polymerization rate (RP ( $\text{s}^{-1}$ )), as the DC at time  $t$  subtracted from the DC at time  $t^{-1}$ . The coefficient of determination was higher than 0.97 for the CA, CA 800 and CLQ curves, whereas it was lower for the CA1200 (0.92) and CTi (0.92) curves; in addition, the latter curve could not be fitted.

### **Diametral tensile strength (DTS)**

The DTS was tested with a universal testing machine (EMIC 2000, Equipamentos e Sistemas de Ensaio, São José dos Pinhais, Brazil) with a 100 kgf load, at a crosshead speed of 1.0  $\text{mm}/\text{min}$ . Standard discs ( $n = 10$ ;  $\text{Ø} = 6 \text{ mm}$ ,  $h = 3 \text{ mm}$ ) were prepared for each experimental group. The sample borders were gently polished with 600-grit abrasive paper. The samples were stored at 37°C and 100% humidity for 24 h. A digital caliper was used to measure the discs before the test. The DTS ( $\sigma$ ) values (MPa) were calculated as follows:

$\sigma = 2P/\pi \times D \times h$ , where  $D$  is diameter,  $h$  is the height, and  $\pi = 3.14$ .

### **Hydrogenic potential**

The evaluation of the hydrogenic potential (pH) was performed at time intervals of 3, 24, 48, 72 h, 7 and 14 days using a digital pH meter (608 Analion PM Plus, Ribeirão Preto, Brazil) calibrated with reference solutions. Standard discs ( $n = 15$ ;  $\text{Ø} = 4 \text{ mm}$ ,  $h = 1 \text{ mm}$ ) were prepared for each experimental group. All the discs were stored individually in Eppendorf microtubes (Sigma-Aldrich) containing 1 mL of distilled water, and stored at 37°C throughout the entire test period.

## Calcium ion release

The calcium ion release was assessed by atomic absorption spectrophotometry (Evolution 260 Bio UV-Visible Spectrophotometer, Thermo Fisher Scientific, Madison, USA) at time intervals of 3 h, 1, 4, 7, 14 and 28 days. Standard discs ( $n = 10$ ;  $\varnothing = 8$  mm,  $h = 1.5$  mm) of each experimental group were stored individually in 1.5 mL distilled water at 37°C throughout the entire test period. The calcium ion release test was performed by placing 10  $\mu$ L of the water inside quartz microtubes with 1 mL of arsenazo (Calcium Arsenazo III, Bioclin, Quibasa Química Básica, Brazil) to obtain the spectrophotometric measurements. The discs were placed into microtubes with fresh, deionized water (1.5 mL), and stored according to the storage time being researched. Absorbance values (Abs) were calculated according to the following equation: calcium release (ppm) = (Sample Abs/Standard Abs)  $\times$  100.

## Water absorption and solubility

Discs ( $n = 10$ ;  $\varnothing = 4$  mm,  $h = 1$  mm) of each experimental group were stored in a glass desiccator at 37°C to dry the specimens, and to obtain a constant mass ( $m_1$ ). The specimens were weighed daily using an analytical balance (AUW 220D, Shimadzu) with 0.0001 g accuracy, until a constant mass was obtained. Then, the surface water was removed from the specimens with filter paper, after storage in deionized water at 37°C for 7 days ( $m_2$ ). The samples were dried again in the desiccator at 37°C to obtain a constant mass ( $m_3$ ). The water solubility ( $WSL = [(m_1 - m_3)/m_3] \times 100$ ) and sorption ( $WSR = [(m_2 - m_3)/m_3] \times 100$ ) were calculated as percentages of the original weight.

## Cell viability

The cytotoxicity assay was performed with an immortalized cell line [L929 mouse fibroblasts] in culture medium (Dulbecco's Modified Eagle's Medium with 4.5 g/L glucose and L-glutamine - DMEM, Lonza, Walkersville, MD, USA) supplemented with 10% fetal bovine serum and 1% antibiotics (10,000 IU/mL of penicillin G and 10,000 mg/mL of streptomycin (Gibco Laboratories, Grand Island, USA), according to ISO 10993-5 (2009). The cells were seeded in culture plates and maintained in an incubator (37°C, 5% CO<sub>2</sub>) until

subconfluence was obtained. Next,  $2 \times 10^4$  cells in 200  $\mu$ L of culture medium were cultured in a 96-well plate and incubated at a controlled temperature of 37°C and pressure, in a humid environment of 95% air and 5% CO<sub>2</sub> for 24 h. After this period, the cells that adhered to the bottom of the culture plate formed a cell monolayer that was deposited on the eluates. These eluates were obtained by simultaneously immersing the standard discs ( $n = 6$ ;  $\varnothing = 5.5$  mm,  $h = 1$  mm) of each material individually in Eppendorf microtubes (Sigma-Aldrich) containing 1 mL of DMEM culture medium, using the same incubation parameters of 37°C and 5% CO<sub>2</sub> for 24 h. The eluates were used to replace the medium in the test wells, and the plate was incubated again for the same time period under the same conditions (37°C, 5% CO<sub>2</sub> for 24 h).

After 24 h, the medium in each well was replaced with 20  $\mu$ L of 3-(4,5-dimethylthiazol-2-yl)-2,5-diphenyl tetrazolium bromide (MTT) solution (2 mg/ml DMEM), and the plate was incubated again for 4 h to trigger the cell metabolism. The cell viability was assessed using the MTT assay, which determines the ability of viable cells to reduce MTT metabolically by mitochondrial succinic dehydrogenase enzyme activity to blue-purple-colored formazan crystals that accumulate in the cytoplasm. After the incubation period, the medium was replaced with 200  $\mu$ L of dimethyl sulfoxide (DMSO) to resuspend the formazan. A positive control (wells with cells without the addition of eluates), a negative control (wells without cells, containing only DMEM), and the individual compounds used in the development of the experimental materials were used in addition to the wells corresponding to each material tested. This plate was analyzed by Universal ELISA reader spectrophotometry (ELX 800; BIO-TEK Instruments, Winooski, VT, USA) at a wavelength of 540 nm. The results were evaluated as cell viability indicators, based on the absorbance values.

## Statistical analysis

Statistical analyses were performed using SPSS software 22.0 (SPSS Inc, Chicago, USA). The Kolmogorov-Smirnov test was applied to evaluate the Gaussian distribution of the data. One-way ANOVA, followed by the Tukey *post hoc* test, was

used to analyze the parametric data of DTS. The Kruskal-Wallis test, followed by the Dunn multiple test, was used to analyze the water absorption and solubility nonparametric data. Moreover, two-way ANOVA, followed by the Tukey *post hoc* test, was used to analyze the parametric data of the calcium ion release. In the analysis of the cytotoxicity assay, one-way ANOVA, followed by the Tukey *post hoc* test, was used for the 24-h data, and the Kruskal-Wallis test, followed by the Dunn Multiple Comparison test,

was used for the 48-h data. The significance level was set at  $\alpha = 0.05$ .

## Results

The micromorphological analysis of the powder showed irregular morphology with particle agglomerates, and varied grain sizes for the CA800, CA1200 and CTi groups (Figure 1). The XRD patterns were used for the crystalline phase analysis of MTA

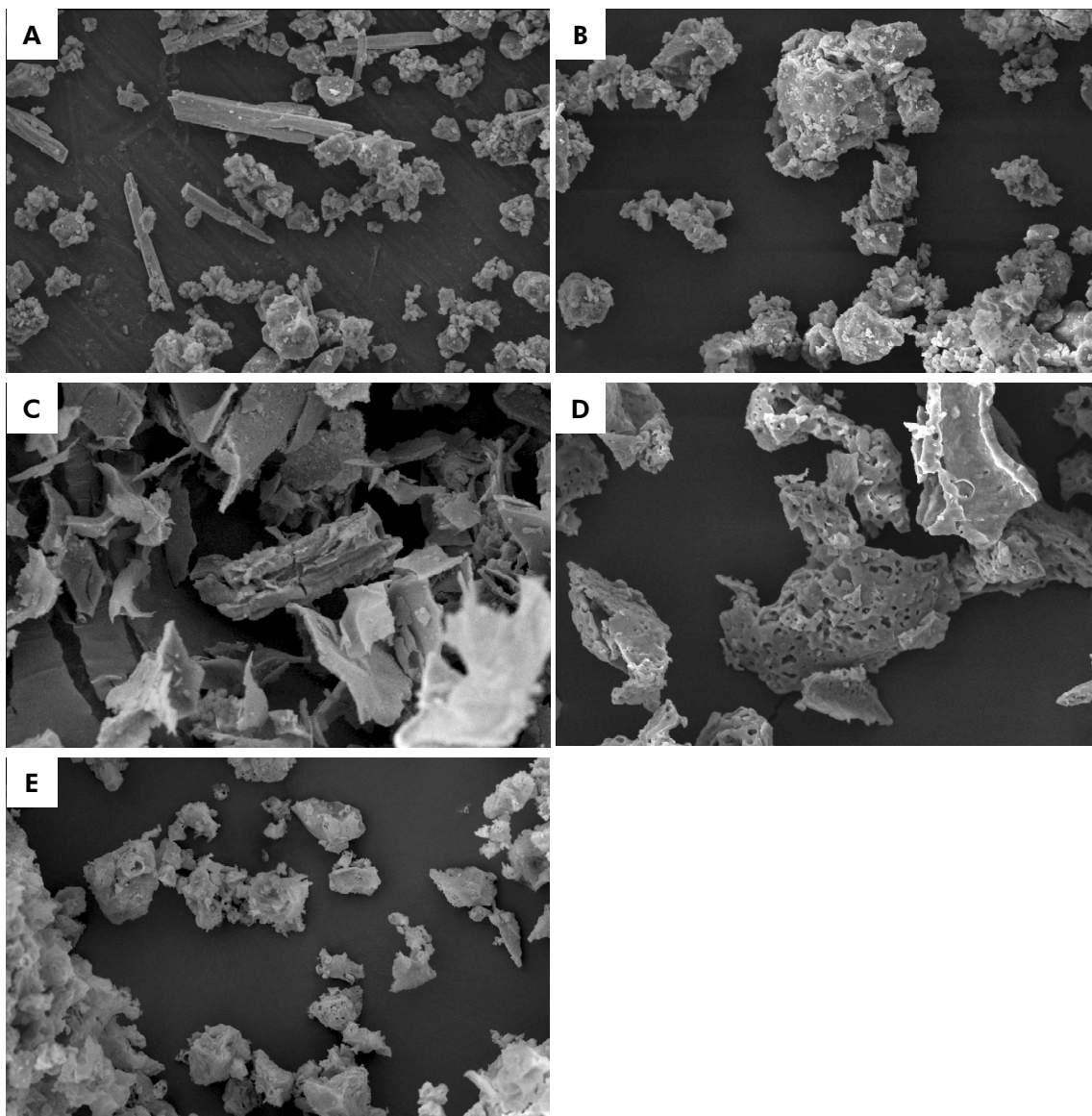


**Figure 1.** SEM images (x1000 magnification) of the particles and grain morphology of the different groups: (a) MTA; (b) CLQ; (c) CA800; (d) CA1200; and (e) CTi.

and CLQ (Figure 2). The presence of tricalcium silicate ( $C_3S$  or  $Ca_3SiO_5$ ) (indicated by the main peaks at  $32.5^\circ$  and  $34.3^\circ$ ) and the dicalcium silicate ( $C_2S$  or  $Ca_2SiO_4$ ) (indicated by the main peaks at  $32.1^\circ$  and  $32.5^\circ$  [Figure 2a]) – was confirmed. The pattern of the MTA powder contained peaks at  $27.4^\circ$ ,  $33.2^\circ$  and  $46.3^\circ$ , representing bismuth oxide ( $Bi_2O_3$ ), and a peak at  $47.6^\circ$  attributed to tricalcium aluminate ( $C_3A$  or  $Ca_3Al_2O_6$ ) (Figure 2a). The crystalline phase analyses of CA calcined at  $800^\circ C$  (CA800) indicated the presence of small crystallites, confirmed by diffused broad bands and minor peaks in the X-ray diffraction pattern (Figure 2b). However, the formation of crystalline phases, mayenite ( $C_{12}A_7$  or  $Ca_{12}Al_{14}O_{33}$ ) and tricalcium aluminate ( $C_3A$  or  $Ca_3Al_2O_6$ ) also occurred in CA calcined at  $1200^\circ C$  (CA1200); the higher intensity

peaks in the XRD patterns indicated larger grains and particles (Figure 2b). The crystalline phase analysis of the CTi powder revealed the presence of calcium titanate indicated by the main peaks at  $32.9^\circ$ ,  $47.0^\circ$  and  $59.2^\circ$  ( $CaTiO_3$ , perovskite). The powder pattern contained peaks at  $37.4^\circ$  and  $53.7^\circ$  representing calcium oxide ( $CaO$ ) and titanium oxide ( $Ti_2O_3$ ), respectively (Figure 2c).

FTIR analysis of the powders confirmed that the crystalline phases of CA calcined at  $800^\circ C$  and  $1200^\circ C$  were similar, and were also similar to those of MTA and CLQ (Figure 2d). Absorption peaks of about  $900-750\text{ cm}^{-1}$  were associated with aluminate phases, whereas those of about  $875\text{ cm}^{-1}$  indicated tricalcium silicate. Intense absorption peaks below  $700\text{ cm}^{-1}$  were also observed, attributed to titanate phases

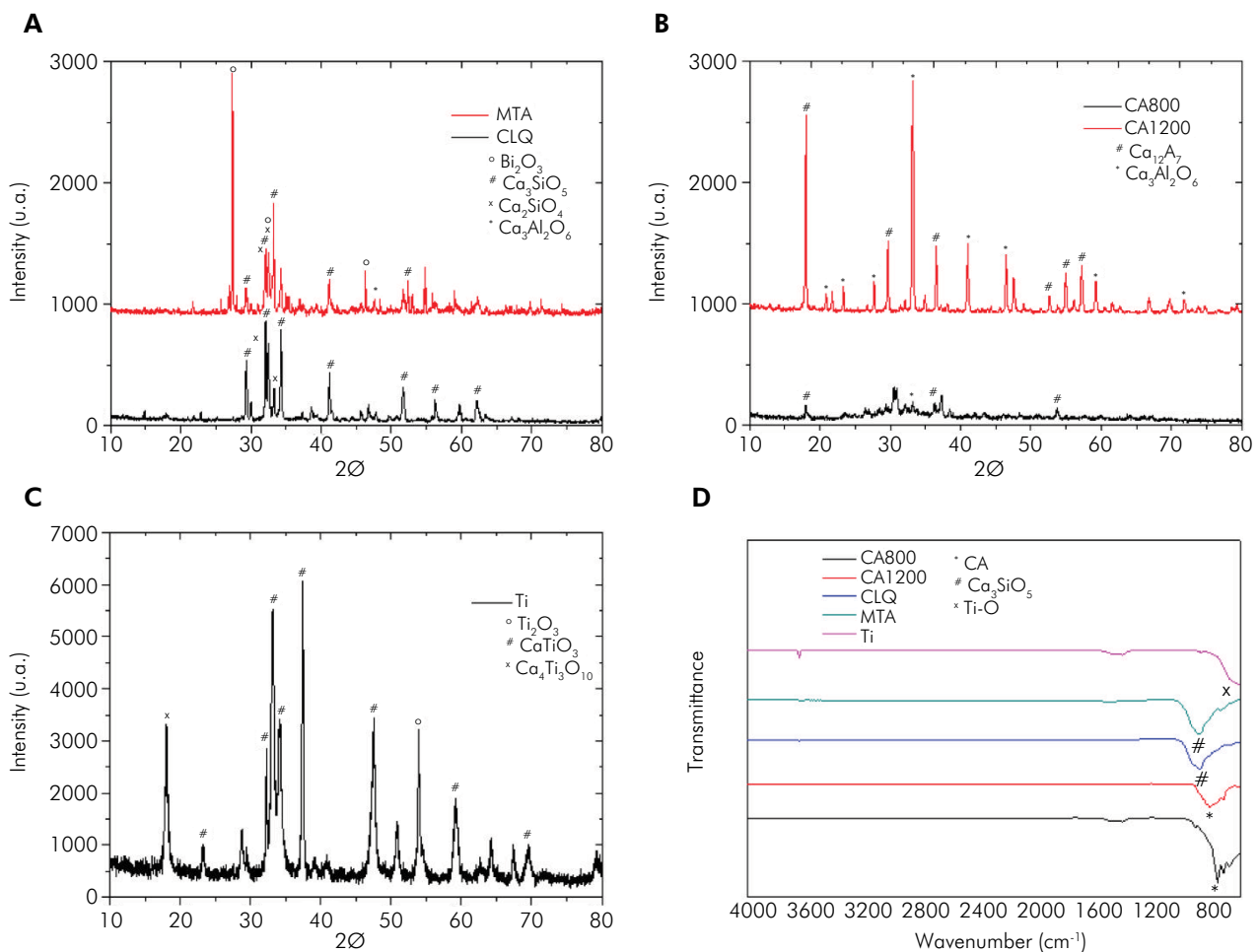


**Figure 2.** Characterization of the crystalline phases using XRD and FTIR: (A) MTA and CLQ (XRD); (B) CA800 and CA 1200 (XRD); (C) CTi (XRD); and (D) all groups (FTIR).

(Figure 2d). The constitution and the proportion of elements after the elemental analysis of the powders were determined by EDX. There was a predominance of calcium in the powders (Table 2).

The DC and rate of polymerization of the experimental materials were the highest for the CLQ and CA 800 groups ( $p < 0.05$ ) (Figure 3). The CA 1200, CTi, and CA groups were unsuitable for use in the light-cure mode (Figure 3). The CLQ, CA800 and CA1200 groups were statistically similar ( $p > 0.05$ ) and showed the highest ( $p < 0.05$ ) DTS values (Table 3).

Regarding water absorption, MTA showed the highest values with no significant difference from CLQ ( $p > 0.05$ ) (Table 3). Regarding water solubility, CA was not significantly different from CA800 and CA1200 ( $p < 0.05$ ) (Table 3). The solubility levels of these two groups were similar to that of MTA ( $p > 0.05$ ).

The solubility of MTA did not significantly differ from that of CLQ and CTi ( $p > 0.05$ ) (Table 3).

All experimental materials showed an alkaline pH value ( $\sim 10.5$ ), with increasing pH values, and calcium ion release over time. After 28 days, the CA group showed the highest mean ion calcium release ( $p < 0.05$ ). On the other hand, CLQ showed the lowest calcium ion release values after 28 days ( $p < 0.05$ ) (Table 4).

Regarding cytotoxicity (Figure 4), CA800 and CA1200 showed 97.6% and 103.8% cell viability, respectively, after 24 h, percentages that were statistically similar to CLQ (105.4%), MTA (116.3%) and the BLD monomer mixture (99%) ( $p > 0.05$ ), but that differed statistically from CTi (63.1%) ( $p < 0.05$ ). After 48 h, the CA800 (88.8%) and CA1200 (81.5%) groups differed statistically from CTi (47.3%) ( $p < 0.05$ ) (Figure 4).

**Table 2.** Results of the elemental analysis of each filler particle.

Material	Ca (%)	Al (%)	Si (%)	Ti (%)	Bi (%)	Fe (%)
MTA	70.3	-	6.1	-	21.4	1.5
CLQ	91.1	-	7.9	-	-	-
CA800	77.5	22.5	-	-	-	-
CA1200	76.5	23.5	-	-	-	-
CTi	76.1	-	-	23.5	-	-

Elemental analysis by energy dispersive X-Ray (EDX) of MTA® and the filler particles, Clinker-Fillapex® (CLQ); CA calcined at 800°C (CA800) and 1200°C (CA1200), and calcium titanate (CTi). Ca (Calcium), Al (Aluminum), Si (Silicon), Ti (Titanate), Bi (Bismuth) and Fe (Iron) are expressed in percentages.

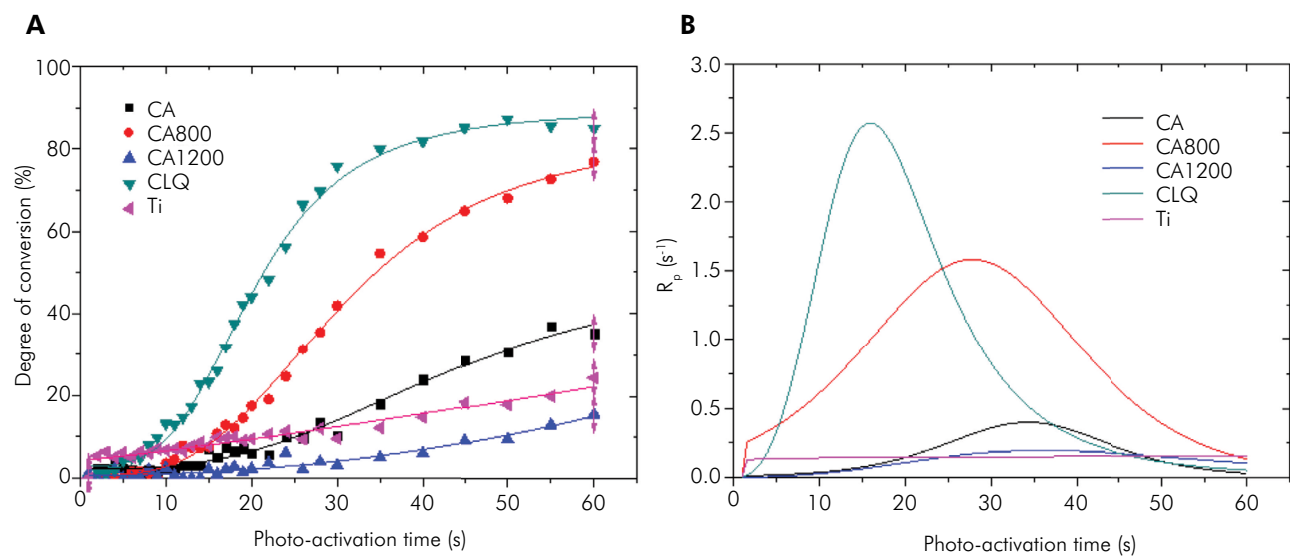


**Figure 3.** (A) DC (%) and (B) rate of polymerization  $R_p$  ( $s^{-1}$ ) profiles of the experimental materials.

**Table 3.** Means ( $\pm$ SD) of the diametral tensile strength (DTS; MPa), and median (1<sup>st</sup>; 3<sup>rd</sup> Quartile) of water absorption ( $W_{SR}$ ; %) and water solubility ( $W_{SL}$ ; %).

Material	DTS	$W_{SR}$	$W_{SL}$
MTA	3.80 (0.58) <sup>a</sup>	3.25 (2.64; 3.43) <sup>a</sup>	-8.37 (-8.54; -7.95) <sup>bcd</sup>
CLQ	5.68 (1.28) <sup>bc</sup>	1.95 (1.63; 2.18) <sup>ab</sup>	-2.69 (-3.17; -1.68) <sup>cd</sup>
CA	4.82 (0.28) <sup>ab</sup>	1.10 (0.60; 1.63) <sup>b</sup>	-17.78 (-18.75; -16.15) <sup>a</sup>
CA800	6.39 (0.99) <sup>c</sup>	0.74 (0.65; 1.10) <sup>b</sup>	-9.96 (-10.08; -9.77) <sup>ab</sup>
CA1200	6.10 (0.93) <sup>c</sup>	0.84 (0.45; 1.14) <sup>b</sup>	-9.58 (-9.90; -8.59) <sup>abc</sup>
CTi	4.44 (0.96) <sup>a</sup>	0.30 (0.01; 0.47) <sup>b</sup>	2.78 (2.26; 3.07) <sup>d</sup>

Different letters indicate a statistically significant difference for each test ( $p < 0.05$ )

**Table 4.** Means ( $\pm$ SD) of calcium ion release (ppm) for materials and time periods.

Material	Time						Cumulative ion release
	3h	1 day	4 days	7 days	14 days	28 days	
MTA	35.47 (3.24) <sup>a,E</sup>	38.17 (4.21) <sup>a,E</sup>	55.79 (2.67) <sup>b,D</sup>	65.92 (6.35) <sup>a,C</sup>	89.01 (3.90) <sup>b,B</sup>	115.38 (2.51) <sup>b,A</sup>	399.74
CLQ	5.80 (0.42) <sup>d,E</sup>	6.93 (13.74) <sup>c,E</sup>	9.67 (0.54) <sup>f,D</sup>	13.25 (2.10) <sup>d,C</sup>	18.32 (2.46) <sup>e,B</sup>	22.91 (2.86) <sup>e,A</sup>	76.88
CA	34.01 (3.93) <sup>a,D</sup>	34.62 (2.54) <sup>a,D</sup>	63.60 (3.76) <sup>a,C</sup>	66.97 (4.65) <sup>a,C</sup>	95.48 (3.45) <sup>a,B</sup>	124.30 (3.81) <sup>a,A</sup>	418.98
CA800	10.86 (2.37) <sup>c,D</sup>	8.81 (2.65) <sup>c,D</sup>	14.12 (2.02) <sup>e,C</sup>	15.29 (0.83) <sup>d,BC</sup>	17.48 (1.76) <sup>e,B</sup>	25.10 (2.31) <sup>e,A</sup>	91.66
CA1200	21.53 (2.81) <sup>b,C</sup>	21.83 (2.61) <sup>b,C</sup>	24.04 (3.25) <sup>d,BC</sup>	25.75 (2.32) <sup>c,B</sup>	26.76 (2.75) <sup>d,B</sup>	34.18 (2.43) <sup>d,A</sup>	154.09
CTi	24.31 (0.97) <sup>b,E</sup>	24.70 (1.86) <sup>b,E</sup>	29.06 (2.87) <sup>c,D</sup>	34.28 (3.23) <sup>b,C</sup>	41.42 (1.98) <sup>c,B</sup>	53.15 (3.50) <sup>c,A</sup>	206.92

Different lowercase letters in columns and uppercase letters in rows indicate statistically significant differences ( $p < 0.05$ )

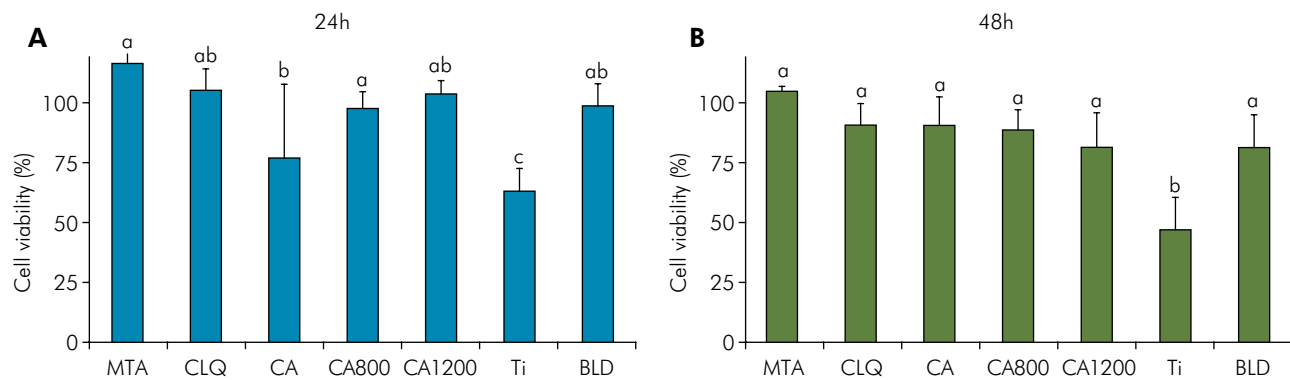


**Figure 4.** Mean ( $\pm$  SD) cell viability (%) after 24 h (A) and 48 h (B). The cell control was considered equal to 100%. Different letters indicate statistically significant differences ( $p < 0.05$ ). BLD is a mixture of 50% Bis-EMA 10 and 50% PEG 400. \*Statistically similar to the cell control ( $p > 0.05$ ).

## Discussion

The characterization of the inorganic particles revealed a mixture of phases resulting from the synthesis process. Preparation of the CA powder by solution combustion synthesis, using only urea as the fuel, produced a mixture of CA phases, C<sub>3</sub>A and

C<sub>12</sub>A<sub>7</sub><sup>28</sup> and additional annealing promoted the degree of crystallinity, grain growth and formation of the CA crystalline phases.<sup>25</sup> Similarly, the chemical method used to synthesize CaTiO<sub>3</sub> perovskite generated amorphous carbon powders from residual organic compounds, pulverized citric acid, and ethylene glycol. The microwave oven system used for annealing

promoted rapid phase formation, which was related to  $\text{TiO}_2$  formation; the MTA and CLQ groups also showed a mixture of phases, which could be observed in micrographs of the MTA powder (Figure 2b). Therefore, this condition was balanced between the samples. However, it may have led to some differences in the test results (Figure 2).

The polymerization kinetic results indicated the highest DC and rate of polymerization values for CLQ and CA800, respectively. Since the tested materials consisted of the same polymeric matrix, this difference could be explained by the filler particles. All the diffraction peaks were attributed to the phase described, as corroborated by the literature.<sup>29</sup> Pastes with smaller crystalline phases (CLQ and CA800) showed better results in terms of DC and polymerization rates (Figure 3), as confirmed by the broad diffusion bands and minor peaks in the X-ray diffraction pattern (Figure 1). This could be attributed to a light-scattering effect in the materials that showed the poorest results, caused by non-agglomerated larger-sized particles. Thus, a possible attenuation in the light intensity may have decreased the DC and polymerization rate.<sup>30</sup> Furthermore, although calcium aluminate was used in the different pastes, there was a substantial change in the results, because the factors previously described were related to the calcination temperature, which promoted the difference in particle size and phase distribution.<sup>25,28</sup>

DTS was used to evaluate the physical properties of the experimental materials, so that these materials could be reused in future clinical applications. Materials used in VPT are subjected to significant load during restorative procedures.<sup>22</sup> The performance of MTA and CTi was similar to that of CA, according to the DTS results (Table 3). CA1200, CA800, and CLQ had superior DTS results (Table 3), in agreement with a previous study.<sup>22</sup> These results showed how a ternary photoinitiation system (DHEPT, EDAB and camphorquinone) can be used to boost the potential of the dual-cure system to improve the mechanical properties. Moreover, the good mechanical properties of the calcium aluminate can be attributed to the presence of CA phases (mainly  $\text{C}_{12}\text{A}_7$ ), which hydrate rapidly, thus improving the material setting time.<sup>20-</sup>  
<sup>21</sup> In particular, CA800 contained small crystallites,

as shown by the broad diffusion bands and low peak heights in the X-ray diffraction pattern. On other hand, the CA1200 material had lower CA1200 content than the CA material, but CA1200 showed higher DTS than CA. This is because there is no fluoride ytterbium in the CA material. Fluoride ytterbium was added with the silanization treatment. The addition of a filler with a bonding agent turns the polymer blend into a rigid resin composite after light-curing. The organosilane cohesive bonding promotes higher mechanical properties than any type of absorption or adsorption from the aluminate or titanate fillers.<sup>31</sup>

All the tested materials showed good potential for alkalizing the environment ( $\text{pH} \approx 10.5$ ). Although the values were slightly higher than those found in other studies,<sup>22,32</sup> the results showed a tendency towards stabilizing the pH values, which reflected the higher dimensional stability of the resinous materials.<sup>19,22</sup> An alkalizing environment can increase the proliferation of human dental pulp cells<sup>33</sup> and stimulate the formation of calcified barriers, promoting stem cell differentiation capable of forming mineralized tissues.<sup>34</sup> The hydrogenic potential (pH) results suggested that all the experimental resin-based dual-cured materials were promising for promoting growth factor release from dentin. It is important to highlight that VPT stimulates the formation of dentine, and maintains dental pulp vitality. Thus, growth factor release from dentin is important for pulp repair and maintenance of antimicrobial effects.<sup>35</sup>

Calcium ion release could also contribute to this reparative effect, since calcium can stimulate the formation of hard tissues through osteoblast differentiation, proliferation and odontogenic expression.<sup>15,18</sup> These properties are important to induce dentin formation in human teeth subjected to VPT.<sup>16,18,19</sup> The results showed that calcium ion release occurred due to the predominance of calcium in the powders of the pastes, and an increasing release was observed over the time intervals of evaluation for all the groups (Table 4). The highest calcium ion release values for CA, Ti, and CA1200 could be related to these materials having the lowest DC (Figure 3). Furthermore, the mass fraction of calcium sulfide is higher in CA than in the other tested materials (except MTA), thus improving the calcium ion release. The calcium aluminate obtained at 800°C

(CA800) had a smaller size and a lower number of crystalline particles, which could facilitate the calcium release. On the other hand, CA1200 had the largest size and highest number of crystalline particles, as confirmed by the broad diffusion bands and the higher peak heights in the X-ray diffraction pattern (Figure 2). The high calcium ion release could be related to the homeostatic mechanisms of the cells in regulating the intracellular calcium levels in VPT.<sup>36</sup>

The materials tested showed high solubility (Table 3), except CTi and CLQ, because of their ability to release calcium ions (Table 4). In general, the groups had low sorption values, probably due to the higher dimensional stability of resinous materials.<sup>22</sup> Some hydrophilic components, such as resin molecules that contain hydrophilic moieties, increased the sorption and solubility, as observed in all the groups, since the experimental materials (pastes) tested contained the same monomeric composition (Bis-EMA 10, Bis-EMA 30 and PEG 400). The significant differences between the sorption and solubility values of these groups could be explained by the differences in the inorganic particles. A large filler particle size and consequently low monomeric content resulted in a reduction in the sorption and solubility.<sup>37</sup>

The cell viability data showed an equivalent performance of CA800, CA1200 and MTA after 24 h and 48 h, thus suggesting the potentially similar biocompatibility of these materials. The biocompatibility was enhanced by the resin component, attributed to its lower diffusion characteristics, which showed the best result in this test. Furthermore, it is suggested that calcium ion release, ionic activities, toxic components and pH changes may affect the behavior of the cells.<sup>38</sup> Similar cell viability values in the presence of MTA in an 24-h evaluation can be found in the literature.<sup>37</sup> However, the cell viability decreased as the evaluation period increased.<sup>39</sup> The good performance of CA800, CA1200 and CLQ is a consequence of their high dimensional stability and stable post-setting pH.<sup>22</sup>

Although L929 fibroblasts have been used in studies<sup>40</sup> and are established by ISO 10993:2009, the results of the present study should be analyzed carefully. The type of cell used can cause variable cytotoxicity results, since other cells can be found in endodontic treatments.

In general, the results showed the potential of the experimental materials, in comparison with the key physicochemical and biological properties of MTA. The incorporation of calcium aluminate into MTA-based materials showed promising results with properties similar or superior to MTA. An important advantage of using dual-cured pulp capping materials is that the procedure is simple, since it requires only two steps, and fast, since it is not necessary to wait for the setting time to elapse. Moreover, dual-cured calcium aluminate- and calcium titanate-based materials still have the potential advantage of bonding with resin composites.<sup>23</sup> A limitation of this study was that only *in vitro* evaluations were performed, and future *in vivo* and clinical studies should be conducted to provide stronger evidence of the potentially beneficial effect of using these materials for VPT. Furthermore, other biological properties important for biomaterials, such as gene expression and protein levels, should be evaluated in future studies. There are a limited number of independent studies regarding the development and evaluation of resin-based dual-cured calcium aluminate and calcium titanate materials for endodontic treatments, and this study demonstrated their potential use for VPT.

## Conclusions

Calcium aluminate and calcium titanate used as filler particles in resin with high-molecular weight monomers have the potential to create a suitable pulp capping agent for VPT. The experimental dual-cured calcium aluminate- and calcium titanate-based materials showed physicochemical and biological properties similar to those of MTA.

## References

1. Giraud T, Jeanneau C, Rombouts C, Bakhtiar H, Laurent P, About I. Pulp capping materials modulate the balance between inflammation and regeneration. *Dent Mater*. 2019 Jan;35(1):24-35. <https://doi.org/10.1016/j.dental.2018.09.008>

2. Silva AF, Marques MR, Rosa WL, Tarquinio SB, Rosalen PL, Barros SP. Biological response to self-etch adhesive after partial caries removal in rats. *Clin Oral Investig*. 2018 Jul;22(6):2161-73. <https://doi.org/10.1007/s00784-017-2303-z>
3. Hilton TJ. Keys to clinical success with pulp capping: a review of the literature. *Oper Dent*. 2009 Sep-Oct;34(5):615-25. <https://doi.org/10.2341/09-132-0>
4. da Rosa WL, Cocco AR, Silva TM, Mesquita LC, Galarça AD, Silva AF, et al. Current trends and future perspectives of dental pulp capping materials: A systematic review. *J Biomed Mater Res B Appl Biomater*. 2018 Apr;106(3):1358-68. <https://doi.org/10.1002/jbm.b.33934>
5. Prati C, Gandolfi MG. Calcium silicate bioactive cements: biological perspectives and clinical applications. *Dent Mater*. 2015 Apr;31(4):351-70. <https://doi.org/10.1016/j.dental.2015.01.004>
6. Qureshi A, e S, Nandakumar, Pratapkumar, Sambashivarao. Recent advances in pulp capping materials: an overview. *J Clin Diagn Res*. 2014 Jan;8(1):316-21. <https://doi.org/10.7860/JCDR/2014/7719.3980>
7. Erfanparast L, Iranparvar P, Vafaei A. Direct pulp capping in primary molars using a resin-modified Portland cement-based material (TheraCal) compared to MTA with 12-month follow-up: a randomised clinical trial. *Eur Arch Paediatr Dent*. 2018 Jun;19(3):197-203. <https://doi.org/10.1007/s40368-018-0348-6>
8. Camilleri J. Characterization of hydration products of mineral trioxide aggregate. *Int Endod J*. 2008 May;41(5):408-17. <https://doi.org/10.1111/j.1365-2591.2007.01370.x>
9. Ranjesh B, Isidor F, Dalstra M, Løvschall H. Diametral tensile strength of novel fast-setting calcium silicate cement. *Dent Mater J*. 2016;35(4):559-63. <https://doi.org/10.4012/dmj.2015-390>
10. Bakhtiar H, Aminishakib P, Ellini MR, Mosavi F, Abedi F, Esmailian S, et al. Dental pulp response to retroMTA after partial pulpotomy in permanent human teeth. *J Endod*. 2018 Nov;44(11):1692-6. <https://doi.org/10.1016/j.joen.2018.07.013>
11. Parirokh M, Torabinejad M. Mineral trioxide aggregate: a comprehensive literature review—Part I: chemical, physical, and antibacterial properties. *J Endod*. 2010 Jan;36(1):16-27. <https://doi.org/10.1016/j.joen.2009.09.006>
12. Mente J, Geletneky B, Ohle M, Koch MJ, Friedrich Ding PG, Wolff D, et al. Mineral trioxide aggregate or calcium hydroxide direct pulp capping: an analysis of the clinical treatment outcome. *J Endod*. 2010 May;36(5):806-13. <https://doi.org/10.1016/j.joen.2010.02.024>
13. Schwendicke F, Brouwer F, Stolpe M. Calcium hydroxide versus mineral trioxide aggregate for direct pulp capping: a cost-effectiveness analysis. *J Endod*. 2015 Dec;41(12):1969-74. <https://doi.org/10.1016/j.joen.2015.08.019>
14. Da Costa J, Lubisich E, Ferracane J, Hilton T. Comparison of efficacy of an in-office whitening system used with and without a whitening priming agent. *J Esthet Restor Dent*. 2011 Apr;23(2):97-104. <https://doi.org/10.1111/j.1708-8240.2010.00400.x>
15. Vitti RP, Pacheco RR, Silva EJ, Prati C, Gandolfi MG, Piva E, et al. Addition of phosphates and chlorhexidine to resin-modified MTA materials. *J Biomed Mater Res B Appl Biomater*. 2019 Aug;107(6):2195-201. <https://doi.org/10.1002/jbm.b.34315>
16. Gomes-Filho JE, de Moraes Costa MT, Cintra LT, Lodi CS, Duarte PC, Okamoto R, et al. Evaluation of alveolar socket response to Angelus MTA and experimental light-cure MTA. *Oral Surg Oral Med Oral Pathol Oral Radiol Endod*. 2010 Nov;110(5):e93-7. <https://doi.org/10.1016/j.tripleo.2010.05.065>
17. Shin JH, Jang JH, Park SH, Kim E. Effect of mineral trioxide aggregate surface treatments on morphology and bond strength to composite resin. *J Endod*. 2014 Aug;40(8):1210-6. <https://doi.org/10.1016/j.joen.2014.01.027>
18. Gandolfi MG, Siboni F, Prati C. Chemical-physical properties of TheraCal, a novel light-curable MTA-like material for pulp capping. *Int Endod J*. 2012 Jun;45(6):571-9. <https://doi.org/10.1111/j.1365-2591.2012.02013.x>
19. Formosa LM, Mallia B, Camilleri J. The chemical properties of light- and chemical-curing composites with mineral trioxide aggregate filler. *Dent Mater*. 2013 Feb;29(2):e11-9. <https://doi.org/10.1016/j.dental.2012.11.006>
20. Jefferies S. Bioactive and biomimetic restorative materials: a comprehensive review. Part II. *J Esthet Restor Dent*. 2014 Jan-Feb;26(1):27-39. <https://doi.org/10.1111/jerd.12066>
21. Almeida LH, Moraes RR, Morgental RD, Cava SS, Rosa WL, Rodrigues P, et al. Synthesis of silver-containing calcium aluminate particles and their effects on a MTA-based endodontic sealer. *Dent Mater*. 2018 Aug;34(8):e214-23. <https://doi.org/10.1016/j.dental.2018.05.011>
22. Dantas RV, Conde MC, Sarmento HR, Zanchi CH, Tarquinio SB, Ogliari FA, et al. Novel experimental cements for use on the dentin-pulp complex. *Braz Dent J*. 2012;23(4):344-50. <https://doi.org/10.1590/S0103-64402012000400006>
23. Ruiz JL, Mitra S. Using cavity liners with direct posterior composite restorations. *Compend Contin Educ Dent*. 2006 Jun;27(6):347-51.
24. Zanchi CH, Münchow EA, Ogliari FA, Chersoni S, Prati C, Demarco FF, et al. Development of experimental HEMA-free three-step adhesive system. *J Dent*. 2010 Jun;38(6):503-8. <https://doi.org/10.1016/j.jdent.2010.03.006>
25. Cava S, Tebcherani SM, Souza IA, Pianaro SA, Paskocimas CA, Longo E, et al. Structural characterization of phase transition of Al<sub>2</sub>O<sub>3</sub> nanopowders obtained by polymeric precursor method. *Mater Chem Phys*. 2007;103(2-3):394-9. <https://doi.org/10.1016/j.matchemphys.2007.02.046>
26. Delbrücke T, Gouvêa RA, Moreira ML, Raubach CW, Varela JA, Longo E, et al. Sintering of porous alumina obtained by biotemplate fibers for low thermal conductivity applications. *J Eur Ceram Soc*. 2013;33(6):1087-92. <https://doi.org/10.1016/j.jeurceramsoc.2012.11.009>

27. Mazzo TM, Oliveira LM, Macario LR, Avansi Junior W, André RS, Rosa IL, et al. Photoluminescence properties of  $\text{CaTiO}_3:\text{Eu}^{3+}$  nanophosphor obtained by the polymeric precursor method. *Mater Chem Phys*. 2014;145(1-2):141-50. <https://doi.org/10.1016/j.matchemphys.2014.01.051>
28. Ianoş R, Lazău I, Păcurariu C, Barvinschi P. Fuel mixture approach for solution combustion synthesis of  $\text{Ca}_3\text{Al}_2\text{O}_6$  powders. *Cement Concr Res*. 2009;39(7):566-72. <https://doi.org/10.1016/j.cemconres.2009.03.014>
29. Chang KC, Chang CC, Huang YC, Chen MH, Lin FH, Lin CP. Effect of tricalcium aluminate on the physicochemical properties, bioactivity, and biocompatibility of partially stabilized cements. *PLoS One*. 2014 Sep;9(9):e106754. <https://doi.org/10.1371/journal.pone.0106754>
30. Silva EM, Poskus LT, Guimarães JG. Influence of light-polymerization modes on the degree of conversion and mechanical properties of resin composites: a comparative analysis between a hybrid and a nanofilled composite. *Oper Dent*. 2008 May-Jun;33(3):287-93. <https://doi.org/10.2341/07-81>
31. Halvorson RH, Erickson RL, Davidson CL. The effect of filler and silane content on conversion of resin-based composite. *Dent Mater*. 2003 Jun;19(4):327-33. [https://doi.org/10.1016/S0109-5641\(02\)00062-3](https://doi.org/10.1016/S0109-5641(02)00062-3)
32. Vitti RP, Prati C, Sinhoretta MA, Zanchi CH, Souza E Silva MG, Ogliari FA, et al. Chemical-physical properties of experimental root canal sealers based on butyl ethylene glycol disalicylate and MTA. *Dent Mater*. 2013 Dec;29(12):1287-94. <https://doi.org/10.1016/j.dental.2013.10.002>
33. Takita T, Hayashi M, Takeichi O, Ogiso B, Suzuki N, Otsuka K, et al. Effect of mineral trioxide aggregate on proliferation of cultured human dental pulp cells. *Int Endod J*. 2006 May;39(5):415-22. <https://doi.org/10.1111/j.1365-2591.2006.01097.x>
34. Rosa V, Zhang Z, Grande RH, Nör JE. Dental pulp tissue engineering in full-length human root canals. *J Dent Res*. 2013 Nov;92(11):970-5. <https://doi.org/10.1177/0022034513505772>
35. Neunzehn J, Pötschke S, Hannig C, Wiesmann HP, Weber MT. Odontoblast-like differentiation and mineral formation of pulpsphere derived cells on human root canal dentin in vitro. *Head Face Med*. 2017 Dec;13(1):23. <https://doi.org/10.1186/s13005-017-0156-y>
36. Nicotera P, Bellomo G, Orrenius S. Calcium-mediated mechanisms in chemically induced cell death. *Annu Rev Pharmacol Toxicol*. 1992;32(1):449-70. <https://doi.org/10.1146/annurev.pa.32.040192.002313>
37. Silva EJ, Herrera DR, Rosa TP, Duque TM, Jacinto RC, Gomes BP, et al. Evaluation of cytotoxicity, antimicrobial activity and physicochemical properties of a calcium aluminate-based endodontic material. *J Appl Oral Sci*. 2014 Jan-Feb;22(1):61-7. <https://doi.org/10.1590/1678-775720130031>
38. Gandolfi MG, Ciapetti G, Taddei P, Perut F, Tinti A, Cardoso MV, et al. Apatite formation on bioactive calcium-silicate cements for dentistry affects surface topography and human marrow stromal cells proliferation. *Dent Mater*. 2010 Oct;26(10):974-92. <https://doi.org/10.1016/j.dental.2010.06.002>
39. Poggio C, Arciola CR, Beltrami R, Monaco A, Dagna A, Lombardini M, et al. Cytocompatibility and antibacterial properties of capping materials. *ScientificWorldJournal*. 2014;2014:181945. <https://doi.org/10.1155/2014/181945>
40. Benetti F, Queiroz IOA, Oliveira PH, Conti LC, Azuma MM, Oliveira SH, et al. Cytotoxicity and biocompatibility of a new bioceramic endodontic sealer containing calcium hydroxide. *Braz Oral Res*. 2019;33:e042. <https://doi.org/10.1590/1807-3107bor-2019.vol33.0042>